ORIGINAL PAPER

Syntheses and characterization of vitamin B$_{12}$–Pt(II) conjugates and their adenosylation in an enzymatic assay

Pilar Ruiz-Sánchez · Stefan Mundwiler ·
Bernhard Spingler · Nicole R. Buan ·
Jorge C. Escalante-Semerena · Roger Alberto

Abstract Aiming at the use of vitamin B$_{12}$ as a drug delivery carrier for cytotoxic agents, we have reacted vitamin B$_{12}$ with *trans*-[PtCl(NH$_3$)$_2$(H$_2$O)]$^+$, [PtCl$_3$(NH$_3$)]$^-$ and [PtCl$_4$]$^{2-}$. These Pt(II) precursors coordinated directly to the Co(III)-bound cyanide, giving the conjugates [{Co}– CN–{*trans*-PtCl(NH$_3$)$_2$}]$^+$ (**5**), [{Co}–CN–{*trans*-PtCl$_2$ (NH$_3$)}] (**6**), [{Co}–CN–{*cis*-PtCl$_2$(NH$_3$)}] (**7**) and [{Co}– CN–{PtCl$_3$}]$^-$ (**8**) in good yields. Spectroscopic analyses for all compounds and X-ray structure elucidation for **5** and **7** confirmed their authenticity and the presence of the central "Co–CN–Pt" motif. Applicability of these hetero-dinuclear conjugates depends primarily on serum stability. Whereas **6** and **8** transmetallated rapidly to bovine serum albumin proteins, compounds **5** and **7** were reasonably stable. Around 20% of cyanocobalamin could be detected after 48 h, while the remaining 80% was still the respective vitamin B$_{12}$ conjugates. Release of the platinum complexes from vitamin B$_{12}$ is driven by intracellular reduction of Co(III) to Co(II) to Co(I) and subsequent adenosylation by the adenosyltransferase CobA. Despite bearing a rather large metal complex on the β-axial position, the cobamides in **5** and **7** are recognized by the corrinoid adenosyltransferase enzyme that catalyzes the formation of the organometallic C–Co bond present in adenosylcobalamin after release of the Pt(II) complexes. Thus, vitamin B$_{12}$ can potentially be used for delivering metal-containing compounds into cells.

Keywords Cisplatin · Vitamin B$_{12}$ · Targeting · Adenosyltransferase

P. Ruiz-Sánchez · S. Mundwiler · B. Spingler · R. Alberto (✉)
Institute of Inorganic Chemistry,
University of Zurich,
Winterthurerstrasse 190,
8057 Zurich, Switzerland
e-mail: ariel@aci.uzh.ch

N. R. Buan · J. C. Escalante-Semerena
Department of Bacteriology,
University of Wisconsin,
1550 Linden Dr,
Madison, WI 53706, USA
e-mail: escalante@bact.wisc.edu

Introduction

Cyanocobalamin (aka vitamin B$_{12}$; hereafter referred to as B$_{12}$) is an essential nutrient for most organisms, including humans. Adenosylcobalamin (AdoCbl, aka coenzyme B$_{12}$), the biologically active form of B$_{12}$, is necessary for the function of enzymes involved in diverse physiological processes [1]. In humans, B$_{12}$ is taken up from the intestine and is bound to the protein known as intrinsic factor (IF). The recommended dietary allowance for humans is very low (1–5 μg) [2], and insufficient intake of B$_{12}$ leads to severe diseases such as megaloblastic anemia and neurological malfunctions [3, 4]. In humans and higher animals, gastric IF, haptocorrins (HC) and transcobalamins (TC), bind B$_{12}$ and promote its entry into the cell via three distinct cell surface receptors [5]. In plasma, B$_{12}$ is bound to transport proteins TCI (HC) and TCII. The complex between B$_{12}$ and TCII is taken up by TCII receptor-mediated endocytosis. Once inside the cell, the B$_{12}$–TCII complex is degraded inside lysosomes to release B$_{12}$ into the cytoplasm.

To convert B$_{12}$ to AdoCbl, the cell needs to reduce the cobalt ion in the corrin ring from Co(III) to Co(I). The

latter is a strong nucleophile that attacks the 5′C of ATP forming the unique Co–C bond that tethers the 5′-deoxy-adenosine group (Coβ, upper ligand) to the corrin ring, and releases triphosphate as the byproduct of the reaction [6, 7]. In some microorganisms, the corrinoid adenosylation pathway comprises three steps. The first step is the reduction of cob(III)alamin to cob(II)alamin, which is readily achieved nonenzymatically by dihydroflavins (FADH$_2$, FMNH$_2$) in the cytosol [8]. The second step of the pathway is the reduction of cob(II)balamin to cob(I)alamin by reduced flavodoxin, a nonspecific elec-tron-transfer protein [7, 9]. The third step is catalyzed by an ATP:co(I)rrinoid adenosyltransferase enzyme [10]. Ade-nosyltransferase enzymes have been investigated in several organisms [11, 12] and are in particular well studied in the enterobacterium *Salmonella enterica*. Three evolutionarily distinct corrinoid adenosyltransferases have been described in this bacterium, namely, CobA (EC 2.5.1.17), PduO and EutT [13–15]. Unlike with PduO and EutT, a three-dimensional structure of the *S. enterica* CobA enzyme with substrates bound in the active site has been reported [16]. The nonenzymic reduction of Co(III) to Co(II) releases the upper axial ligand, usually a cyanide or a water molecule. Co(III) has been used to directly anchor different types of bioactive molecules to B$_{12}$. In particular, fluorescent and cytotoxic agents have been conjugated via a Co–C bond to B$_{12}$ and their biological behavior has been studied in detail [17–21]. Since the release of cyano group conjugates would occur preferentially in the cell, these compound–B$_{12}$ conjugates would be regarded as prodrugs in which the essential structural features of cobalamin conceal the active drug attached to it. The indispensable need for AdoCbl in fast-proliferating sites such as cancerous cells or microbial infections would allow the use of B$_{12}$ derivatives as an agent for site-specific delivery of drugs [18, 22, 23].

In previously reported work, we described conjugates of B$_{12}$ of the general composition [{Co}–CN–{M}], where {M} represents complexes of rhenium, technetium and platinum bound via the cyano group to B$_{12}$ [24, 25]. Since cisplatin and some of its derivatives are well-established anticancer drugs [26], we decided to use B$_{12}$ as a vehicle to deliver these cytostatic drugs. In this paper, we describe the synthesis and structure of new Pt(II)-complex adducts of B$_{12}$. The monoactivated form of cisplatin, *cis*-[PtCl(NH$_3$)$_2$(H$_2$O)]$^+$ (**1**) bound directly to the cyanide in B$_{12}$ upon formation of [{Co}–CN–{*cis*-PtCl(NH$_3$)$_2$}] (**2**). With use of the same synthetic approach, the reaction of *trans*-[PtCl(NH$_3$)$_2$(H$_2$O)]$^+$ (**3**), [PtCl$_3$(NH$_3$)]$^-$ (**4**) and [PtCl$_4$]$^{2-}$ yielded [{Co}–CN–{*trans*-PtCl(NH$_3$)$_2$}]$^+$ (**5**), [{Co}–CN–{*trans*-PtCl$_2$(NH$_3$)}] (**6**), [{Co}–CN–{*cis*-PtCl$_2$(NH$_3$)}] (**7**) and [{Co}–CN–{PtCl$_3$}]$^-$ (**8**), respectively (Fig. 1).

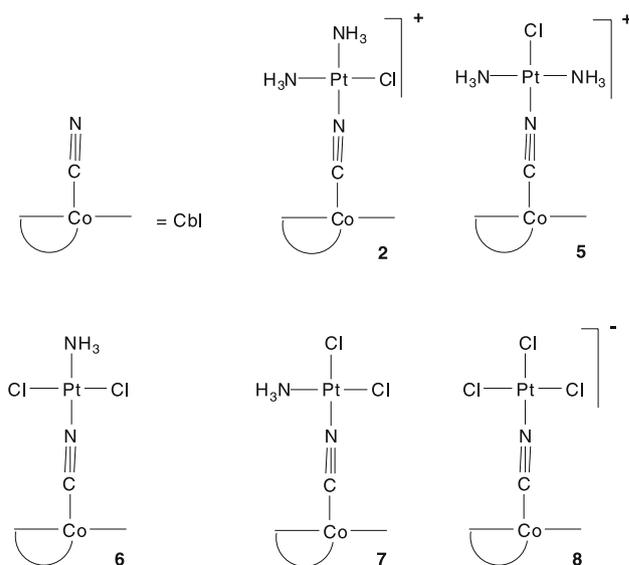Release of Pt(II) complexes inside the cell is crucial for their biological activity. In vitro studies of enzymatic

Fig. 1 Basic structures of vitamin B$_{12}$ (B$_{12}$) adducts with Pt(II) complexes [{Co}–CN–{Pt}]

corrinoid adenosylation by the *S. enterica* CobA enzyme confirmed the hypothesis that upper ligands in conjugates **2**, **5** and **7** were released upon reduction of Co(III) to Co(II) and that the resulting corrinoids were converted to AdoCbl. The Pt(II) complexes (and probably also other ones) were released during this adenosylation process; hence, B$_{12}$-mediated drug uptake and drug release is feasible and B$_{12}$ can act as a site-specific drug carrier.

Materials and methods

General considerations

All chemicals were purchased from Fluka, Sigma, Strem and Acros. Chemicals were of reagent grade and used without further purification. The platinum complex, K[PtCl$_3$(NH$_3$)] was synthesized according to published procedures [27]. All reactions were performed under a nitrogen or argon atmosphere. High-performance liquid chromatography (HPLC) analyses were performed using a Merck–Hitachi L-7000 system equipped with a diode-array UV/vis spectrometer. The following HPLC columns, sol-vent systems and gradients were used: column 1, Macherey Nagel C-18ec RP (5-μm particle size, 100-Å pore size, 250 mm × 3 mm); column 2, Merck C-18e RP Super-sphere® (100-Å pore size, 250 mm × 4 mm); column 3, Bio-Sil® SEC (5-μm particle size, 250-Å pore size, 300 mm × 7.8 mm); solvent system 1, 0.1% AcOH/10% CH$_3$CN in water, pH 3 (solvent A); MeOH (solvent B); solvent system 2, 0.1% trifluoroacetic acid in water (sol-vent A); MeOH (solvent B); solvent system 3, 0.05 M NaH$_2$PO$_4$, 0.05 M Na$_2$HPO$_4$, 0.01 M NaN$_3$, 0.15 M NaCl,

pH 6.8 (solvent A); gradient 1: 0–10 min (100% solvent A), 10–30 min (100% solvent A → 50% solvent A), 30–35 min (50% solvent A → 0% solvent A); gradient 2, 0–5 min (75% solvent A), 5–30 min (75% solvent A → 0% solvent A); gradient 3, 0–15 min (100% solvent A); gradient 4, 0–10 min (100% solvent A), 10–40 min (100% solvent A → 80% solvent A). Preparative HPLC purification was performed using a Varian Prostar system equipped with two Prostar 215 pumps and a Prostar 320 UV/vis detector, using Macherey Nagel Nucleosil C-18ec RP columns (7-μm particle size, 100-Å pore size, 250 mm × 20 mm and 250 mm × 40 mm) and a Waters Xterra Prep RP8 column (5-μm particle size, 100 mm × 30 mm). The fractions were collected and concentrated under a vacuum to eliminate organic solvents and were finally lyophilized. The purity of the final product was analyzed by analytical HPLC. If required, additional preparative HPLC separation was performed until 99% purity was achieved. IR spectra were recorded using a Bio-Rad FTS-45 spectrometer with the samples in compressed KBr pills. NMR spectra were recorded with a Varian Gemini 200 or 300 MHz instrument and a Bruker DRX 500 MHz spectrometer. The chemical shifts are reported relative to residual solvent protons as a reference. The chemical shifts of ^{31}P NMR spectra are relative to orthophosphoric acid in D_2O at 0 ppm. The chemical shifts of ^{195}Pt NMR spectra are relative to K_2PtCl_4 in D_2O at −1,626.4 ppm. Peak assignments of cobalamin derivatives were determined by interpolation of the ^1H correlation spectroscopy and C–H correlation spectra. Crystallographic data were collected using a Stoe IPDS diffractometer at −90 °C using graphite-monochromated Mo Kα radiation (λ = 0.71073 Å). Suitable crystals were covered with Paratone N oil, mounted on top of a glass fiber and immediately transferred to the diffractometer. Eight thousand reflections distributed over the whole limiting sphere were selected by the program SELECT and used for unit cell parameter refinement with the program CELL [28]. Data were corrected for Lorenz and polarization effects as well as for numerical absorption. Structures were solved with direct methods using SIR97 [29] and were refined by full-matrix least-squares methods on F^2 with SHELXL-97 [30]. In the case of **7**, both the amine and the chloride group *cis* to the cyanide are disordered. Because of the high flexibility in that part of the structure, they were refined as two disordered pairs on identical positions each. Therefore, the distances from the platinum to the amine and the chloride *cis* to the cyanide cannot be discussed. Crystallographic data (without structure factors) for the structures reported in this paper have been deposited with the Cambridge Crystallographic Data Centre as supplementary publication nos. CCDC- 655679 and CCDC-655680. Copies of the data can be obtained free of charge from the CCDC (12 Union

Road, Cambridge CB2 1EZ, UK; Tel: +44-1223-336408; Fax: +44-1223-336003; e-mail: deposit@ccdc.cam.ac.uk; Web site: http://www.ccdc.cam.ac.uk). Cyclic voltametry (CV) was carried out using a Metrohm 757 VA Computrace system with a glassy carbon working electrode, a glassy carbon counter electrode and a Ag^+/AgCl reference electrode. All compounds were measured at 1 mM concentrations in 0.1 M $NBu_4[PF_6]$ in methanol, the sweep rate for CV being 0.1 V s^{-1}.

[{Co}–CN–{*trans*-PtCl(NH₃)₂}]⁺

To a mixture of *trans*-[PtCl₂(NH₃)₂] (66 mg, 0.220 mmol) and $AgNO_3$ (38 mg, 0.220 mmol) in the absence of light, 5 mL of H_2O was added. The mixture was stirred overnight and filtrated under N_2. A solution of B_{12} (200 mg, 0.147 mmol) in 15 mL of H_2O was added. The reaction was followed by HPLC measurements (column 1; solvent system 2; gradient 2; flow rate 0.5 mL min^{-1}), and the mixture was stirred for 17 h at 45 °C in the absence of light. The solvent was evaporated off and the crude product purified by preparative HPLC (solvent system 2; gradient 2; flow rate 40 mL min^{-1}) to give **5** as a red powder (184 mg, 77%). X-ray-quality crystals of **5** were prepared by vapor diffusion of acetonitrile into an aqueous solution of **5**. ^1H NMR (500 MHz, D_2O, 20 °C) δ: 0.38 (s, 3H, C20), 0.99–1.09 (m, 2H, C41′, C60′), 1.19 (s, 6H, C46, Pr3), 1.28 (s, 3H, C36), 1.32 (s, 3H, C54), 1.36 (s, 3H, C47), 1.77–2.03 (m, 12H, C42, C60, C48, C30, C25, C41), 2.16–2.20 (d, 6H, B10, B11), 2.35–2.74 (m, 19H, C26, C37, C49, C31, C18, C55, C35, C53, C56), 2.87 (m, 1H, Pr1′), 3.31–3.33 (m, 1H, C13), 3.50–3.71 (m, 9H, C8, Pr1, R5′, NH₃–Pt), 3.86–3.88 (m, 1H, R5), 4.00–4.07 (m, 1H, R4, C19), 4.16–4.23 (m, 3H, C3, Pr2, R2), 4.68 (m, 1H, R3), 6.04 (s, 1H, C10), 6.30 (s, 1H, R1), 6.43 (s, 1H, B4), 6.98 (s, 1H, B2), 7.22 (s, 1H, B7). ^{31}P NMR (200 MHz, D_2O, 20 °C) δ: −1.2. ^{195}Pt NMR (107 MHz, D_2O, 20 °C) δ: −2,350. IR (KBr, cm^{-1}): 2,188. Electrospray ionization mass spectrometry (ESI–MS): 1,697.6 [M + 2Na + $CH_3OH]^+$, 1,619.7 $[M]^+$.

6 and 7

To a mixture of $K[PtCl_3(NH_3)]$ (68 mg, 0.192 mmol) and B_{12} (200 mg, 0.147 mmol), 10 mL of MeOH was added. The reaction was followed by HPLC measurements (column 2; solvent system 1; gradient 1; flow rate 0.4 mL min^{-1}), and the mixture was stirred for 18 h at 45 °C in the absence of light. The solvent was evaporated off and the crude product purified by preparative HPLC (Waters Xterra column; solvent system 1; gradient 4; flow

rate 30 mL min^{-1}). If necessary, a second purification for each product can be done to eliminate free B$_{12}$ (RP-C18 column; solvent system 2; gradient 2; flow rate 40 mL min^{-1}) to give **6** (60 mg, 25%) and **7** (120 mg, 50%) as red powders. X-ray-quality crystals of **7** were prepared by recrystallization of the solid by carefully layering acetone over an aqueous solution of **7** together with NEt$_4$Cl in a NMR tube.

Spectroscopic data for **6**: ^{1}H NMR (500 MHz, CD$_3$OD, 27 °C) δ: 0.43 (s, 3H, C20), 1.19–1.22 (m, 1H, C41), 1.25 (t, 6H, C46, Pr3), 1.40 (s, 3H, C36), 1.48 (m, 6H, C54, C47), 1.72–1.82 (m, 4H, C25, C41), 1.82–2.2 (m, 8H, C42, C60′, C48, C30, C41′), 2.28 (d, 6H, B10, B11), 2.35–2.94 (m, 22H, C26, C37, C49, C31, C18, C55, C35, C53, C56, Pr1′, C60), 3.31–3.33 (m, 1H, C13), 3.66 (m, 1H, C8), 3.75 (m, 2H, Pr1, R5′), 3.92 (s, 1H, R5), 4.10 (m, 1H, R4), 4.23 (m, 2H, R2, C3), 4.29 (d, 1H, C19), 4.36 (m, 1H, Pr2), 4.74 (m, 1H, R3), 6.00 (s, 1H, C10), 6.29 (s, 1H, R1), 6.58 (s, 1H, B4), 7.15 (s, 1H, B2), 7.27 (s, 1H, B7). ^{31}P NMR (200 MHz, D$_2$O, 20 °C) δ: −1.19. ^{195}Pt NMR (107 MHz, D$_2$O, 20 °C) δ: −2,120. IR (KBr, cm^{-1}): 2,200. ESI–MS: 1,662.8 [M + Na + 2H]$^+$, 1,644.9 [M − NH$_3$ + Na + H]$^+$, 1,378.7 [M − Pt − 2Cl − NH$_3$ + Na + H]$^+$.

Spectroscopic data for **7**: ^{1}H NMR (500 MHz, CD$_3$OD, 27 °C) δ: 0.40 (s, 3H, C20), 1.16–1.44 (m, 16H, C46, Pr3, C41′, C42′, C47, C54, C36), 1.71–2.30 (m, 10H, C25, C41, C42, C30, C48, C55, C37), 2.24 (d, 6H, B10, B11), 2.26–2.85 (m, 22H, Pr1, C26, C60, C56, C55′, C37′, C31, C49, C18, C53, C35), 3.20–3.40 (m, 1H, C13), 3.58 (m, 1H, C8), 3.70 (m, 1H, R5′), 3.86 (s, 1H, R5), 4.04 (m, 1H, R4), 4.16 (m, 2H, R2, C3), 4.26 (m, 2H, C19, Pr2), 4.66 (m, 1H, R3), 5.95 (s, 1H, C10), 6.24 (s, 1H, R1), 6.55 (s, 1H, B4), 7.11 (s, 1H, B2), 7.24 (s, 1H, B7). ^{31}P NMR (200 MHz, D$_2$O, 20 °C) δ: −1.19. ^{195}Pt NMR (107 MHz, D$_2$O, 20 °C) δ: −2,120. IR (KBr, cm^{-1}): 2,193. ESI–MS: 1,661.7 [M + Na + H]$^+$, 1,378.7 [M − Pt − 2Cl − NH$_3$ + Na + H]$^+$.

[{Co}–CN–{PtCl$_3$}]$^-$

To a solution of B$_{12}$ (200 mg, 0.147 mmol) in 10 mL of MeOH was added K$_2$[PtCl$_4$] (18 mg, 0.434 mmol). The reaction was followed by HPLC measurements (column 1; solvent system 2; gradient 2; flow rate 0.5 mL min^{-1}), and the mixture was stirred for 10 days at room temperature. The solvent was evaporated and the crude product purified by preparative HPLC (solvent system 2; gradient 2; flow rate 40 mL min^{-1}) to give **8** as a red powder (87 mg, 35%). ^{1}H NMR (500 MHz, D$_2$O, 20 °C) δ: 0.27 (s, 3H, C20), 0.81–0.87 (m, 2H, C41′, C60′), 1.08 (s, 3H, C46), 1.11 (br d, 3H, Pr3), 1.23 (s, 3H, C36), 1.31 (s, 3H, C54), 1.34 (s, 3H, C47), 1.79–1.93 (m, 12H, C42, C60, C48, C30, C25, C41), 2.09 (d, 6H, B10, B11), 2.1–2.2 (m, 2H, C26), 2.3–2.7

(m, 18H, C37, C49, C31, C18, C55, Pr1′, C35, C53, C56), 3.16–3.18 (m, 1H, C13), 3.42 (m, 2H, C8, Pr1), 3.61 (d, 1H, R5′), 3.8 (m, 1H, R5), 3.92 (m, 1H, R4), 3.95 (m, 1H, C19), 4.10–4.12 (m, 3H, C3, Pr2, R2), 4.59 (m, 1H, R3), 5.90 (s, 1H, C10), 6.21 (s, 1H, R1), 6.34 (s, 1H, B4), 6.90 (s, 1H, B2), 7.13 (s, 1H, B7). ^{31}P NMR (200 MHz, D$_2$O, 20 °C) δ: −1.03. ^{195}Pt NMR (107 MHz, D$_2$O, 20 °C) δ: −1,998. IR (KBr, cm^{-1}): 2,198. ESI–MS: 1,735.4 [M + 2Na + CH$_3$OH + H]$^+$, 1,699.4 [M + 2Na + CH$_3$OH − Cl]$^+$, 1,367.5 [M − 2Cl − Pt − Na]$^+$.

Binding of B$_{12}$, **5**, **6**, **7** and **8** to bovine serum albumin

Bovine serum albumin (BSA; 13 mg, 0.2 μmol) was dissolved in phosphate buffer (pH 7.4, 0.1 M, 1 mL). Aliquots of the freshly dissolved cobalamin derivatives (0.2 μmol) were added, and the solutions were stirred at room temperature. Binding to the albumin was measured by HPLC with detection at 360 nm (column 3; solvent system 3; gradient 3; flow rate 1 mL min^{-1}) as was rate of decomposition after 48 h (column 1; solvent system 2; gradient 2; flow rate 0.5 mL min^{-1}). The following amounts of protein-bound cobalamin were found: B$_{12}$, no binding after 6 days; **5**, 5.64% after 4 h, 11.09% after 24 h, 12.33% after 48 h, 15.15% after 74 h; **6**, 30.11% after 4 h, 59.75 after 24 h, 67.07% after 48 h; **7**, 4.73% after 4 h, 11.75% after 24 h, 15.15% after 53 h; **8**, 21.55% after 2 h, 30.35% after 4 h, decomposition after 20 h.

Spectroelectrochemical studies

Reduction of cobalamin derivatives from Co(III) to Co(II) was monitored spectrophotometrically using a Varian Cary 50 spectrometer equipped with a temperature-regulated cuvette holder. The assay mixture (final volume, 7 mL) contained cobalamin (100 μM), MgCl$_2$ (800 μM) and tris(hydroxymethyl)aminomethane (Tris)–Cl buffer (pH 8 at 37 °C, 0.2 M). All experiments were done at 37 °C. The cell was equipped with a platinum net working electrode and a platinum wire counter electrode. Controlled potential coulometry was carried out with an AMEL-549 potentiostat.

Enzymic conversion of B$_{12}$, aqua-cobalamin, **2**, **5** and **7** to AdoCbl

Conversion of cobalamin derivatives to AdoCbl was monitored spectrophotometrically using a PerkinElmer Lambda 45 spectrophotometer equipped with a temperature-regulated cuvette holder. The assay mixtures (final volume, 1 mL) contained cobalamin derivative (50 μM),

MnCl$_2$ or MgCl$_2$ (800 μM), Tris–Cl buffer (pH 8 at 37 °C, 0.2 M), NADPH (500 μM), Fpr (0.08 mg) and FldA (0.08 mg [31]). The reaction mixtures were incubated at 37 °C in the spectrophotometer. Formation of cob(II)al-amin was monitored by the decrease in the absorption of the solution at 525 nm as a function of time. To the pre-vious assay mixtures ATP (400 μM), and CobA (0.04 mg) were added. The reaction mixture was incubated at 37 °C in the spectrophotometer. AdoCbl formation was moni-tored by the increase in the absorption of the solution at 525 nm as a function of time. The products of the corrinoid adenosylation assays were desalted using a C$_{18}$ SepPak cartridge and dried in a SpeedVac concentrator, isolated and analyzed by HPLC with detection at 525 nm. In vitro synthesis of adenosylcorrinoids was assessed in vivo by using strain JE7145 (*metE205 ara-9 eutE18*::MudI1734 *kan$^+$*), JE7179 (*metE205 ara-9 cobA366*::Tn*10*d(*cat$^+$*) *eutE18*::MudI1734 *kan$^+$*), JE6583 (*metE205 ara-9*) or JE1293 (*metE205 ara-9 cobA366*::Tn*10*d(*cat$^+$*)) as an indicator strain in biological activity assays. The cells of the indicator strain grown overnight in 2 mL of nutrient broth were concentrated by centrifugation and washed with 14.5 mM sterile saline; 0.2 mL of the cell suspension (approximately 10^8 cells) was added to 3 mL of molten soft agar and used to overlay a plate of Vogel–Bonner minimal medium containing ethanolamine as a carbon and energy source. The corrinoid standards AdoCbl, B$_{12}$ and aqua-cobalamin (HOCbl; approximately 150 nM) and reaction products were spotted (1 μL) onto the overlay and incubated overnight at 37 °C.

Results and discussion

Synthesis and characterization of 5, 6, 7 and 8

The syntheses of compounds **5**, **6**, **7** and **8** were achieved via a strategy similar to the one described for compound **2** [25]; the yield and the nature of the products were strongly dependent on the Pt(II) precursor used (Scheme 1). The HPLC chromatogram of the reaction between B$_{12}$ and 1.5 equiv of **3** (prepared from *trans*-[PtCl$_2$(NH$_3$)$_2$] with 1 equiv of AgNO$_3$ in water) contained one peak with two different sets of signals in the ^{1}H NMR spectrum. Previously reported work showed that the coordination bond between the benzimidazole base of the nucleotide loop of B$_{12}$ and the Co ion of the ring was broken upon binding to a plat-inum complex [32]. The ^{195}Pt NMR spectrum of the mixture, however, showed only one ^{195}Pt signal at −2,350 ppm. In addition, the IR spectrum contained only one weak characteristic v_{CN} band at 2,188 cm^{-1}, indicating that the platinum complex was bound to the cyanide group in B$_{12}$. The absence of a v_{CN} band at 2,137 cm^{-1},
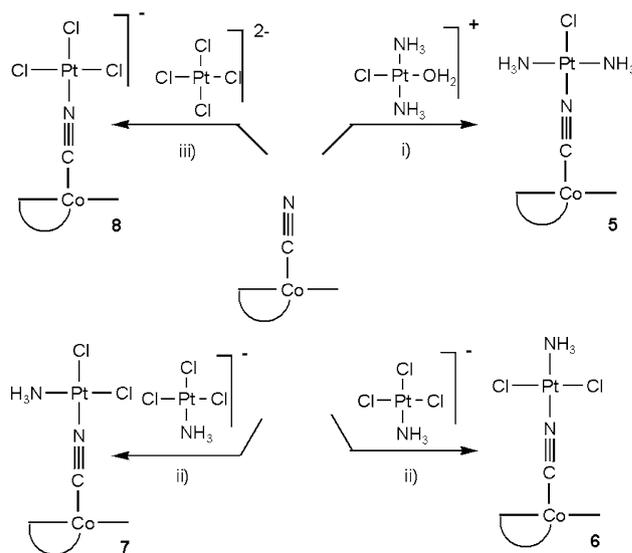
Scheme 1 Reagents and conditions for the preparation of conjugates [{Co}–CN–{Pt}]: *i* with *trans*-[PtCl(NH$_3$)$_2$(H$_2$O)]$^+$ → **5**, MeOH, 17 h at 45 °C, 77%; *ii* with [PtCl$_3$(NH$_3$)]$^-$, MeOH, 18 h at 45 °C, 25% → **6**, 50% → **7**; *iii* with [PtCl$_4$]$^{2-}$, MeOH, 10 days at room temperature, 35% → **8**

indicative for B$_{12}$, further suggested the exclusive coordi-nation of the platinum complex to cyanide. We propose that one of the two species identified by the ^{1}H NMR spectrum is product **5**, in which B$_{12}$ is in the base-on conformation, whereas in the other species the platinum complex is coordinated to cyanide in the protonated base-off conformation. One of the two sets of five signals from 5,6-dimethylbenzimidazole is strongly low-field-shifted (Fig. 2). In base-off AdoCbl, the imidazole proton from the benzimidazole appears at 9.16 ppm [33], whereas the res-onance of the same proton in **5** appears at 9.2 ppm, implying that this set of signals is from **5** in the base-off form. Further evidence for the presence of a base-on and base-off mixture is given by the ^{31}P NMR spectrum, which showed two signals at −1.2 and −1.6 ppm, consistent with B$_{12}$ with an upfield shift of 0.44 ppm upon displacement of the axial benzimidazole base [34].

pH-dependent base-on/base-off equilibria were reported for AdoCbl and other corrins [33]. The nature of the β axial ligand will influence the strength and therefore the release of the Co–N bond to benzimidazole [34, 35]. Accordingly, we observed by ^{1}H NMR measurements that the ratio between the base-on and the base-off products was pH-dependent. After the synthesis of **5** under acidic conditions [to prevent formation of hydroxy-bridged Pt(II) com-plexes], the observed base-off to base-on ratio was about 1:2 in D$_2$O. After addition of base, an almost quantitative and reversible conversion to one single product occurred. This result conclusively confirmed the exclusive binding of
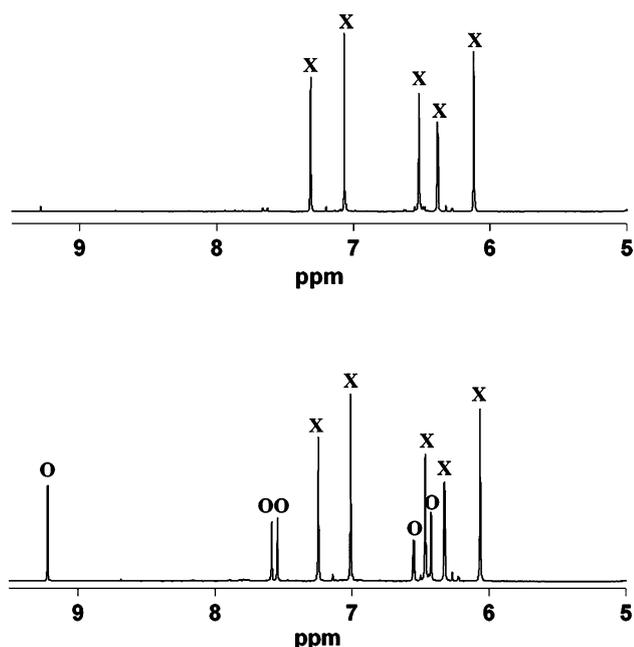
Fig. 2 ^{1}H NMR (500 MHz, CD$_3$OD, 27 °C) spectrum of pure [{Co}–CN–{*trans*-PtCl(NH$_3$)$_2$}]$^+$ (**5**) (*top*) and of a mixture of **5** base-on (*X*) and base-off (*O*) forms (*bottom*). For ease of comparison, only the downfield region from 5 to 9.5 ppm is shown here

3 to the cyanide in B$_{12}$, and was in agreement with the single signal observed in ^{195}Pt NMR measurments.

To estimate the pK_a value of benzimidazole, compound **5** was dissolved in 0.25 M sulfuric acid. The base-off to base-on ratio was about 1:1 (see the supplementary material). From this information we estimated the pK_a value of benzimidazole in **5** to be in the range of 0.4, which compares well with the reported pK_a value of about 0.1 for B$_{12}$ [35].

Following the same synthetic pathway, we directly reacted **4** with B$_{12}$ in water without previous precipitation of one chloride [pathway ii in Scheme 1]. After 4 days of reaction at room temperature, HPLC analysis revealed two new compounds. ^{1}H NMR and ^{31}P NMR data implied a similar product distribution as observed for the formation of **5**, and showed two sets of signals for the desired base-on and for the corresponding base-off forms. As in the case of **5**, the retention times of the base-on and base-off compounds were very similar and they could not be distinguished or separated from each other by preparative HPLC. The reaction did not go to completion in water at room temperature and separation from unreacted B$_{12}$ by preparative HPLC was difficult. On the other hand, in CH$_3$OH or H$_2$O at 45 °C, conversion was quantitative after 18 h. HPLC analysis showed two new and clearly separated peaks, which could be individually isolated by preparative HPLC to yield **6** and **7**. Compounds **6** and **7** were characterized by positive-ion ESI-MS, with observation of the characteristic [M + H + Na]$^+$ and [B$_{12}$ + Na]$^+$ peaks for **6** and [M + 2H + Na]$^+$, [M − NH$_3$ + H +

Na]$^+$ and [B$_{12}$ + Na]$^+$ for **7**, respectively (see the supplementary material). According to the *trans*-effect series, chloride substitution *trans* to a further chloride would be expected, resulting in the preferential formation of compound **7**. Indeed, compound **7** was the main product of the reaction, with about 50% yield. The second product was the *trans* isomer **6** (approximately 30% yield) in which the chloride *trans* to the single NH$_3$ ligand was replaced by B$_{12}$. The IR spectra of **6** and **7** showed ν_{CN} stretching vibrations at 2,200 cm^{-1} and at 2,193 cm^{-1}, respectively. The blueshifts as compared with free B$_{12}$ (2,137 cm^{-1}) are characteristic and indicative for bridging cyanides [36]. Furthermore, the ^{195}Pt NMR spectrum gave a broad peak at −2,120 ppm for both compounds, a region in which signals of cisplatin- or transplatin-like complexes are usually observed.

These assumed authenticities could be confirmed by X-ray structure analysis. Suitable crystals of complex **5** were grown by H$_2$O/CH$_3$CN vapor diffusion and for complex **7** from H$_2$O/Et$_4$NCl/acetone in NMR tubes by solvent layering. For **5** and **7**, the base-on form was found to crystallize exclusively. An ORTEP presentation of **5** is given in Fig. 3 and for **7** in Fig. 4. Crystallographic data are presented in Table 1 and in the supplementary material. The ratios of the cell axes are 1.43 and 1.40 for *b/a* and 1.63 and 1.65 for *c/a* in the structures of **5** and **7**, respectively. These ratios allow a classification of B$_{12}$ crystal structures into different clusters. Here, both **5** and **7** belong to cluster II, the same cluster as recently found for B$_{12}$ derivatives with metal chelating ligands bound to the corrin ring [37].

With respect to application of these "platinated" B$_{12}$ derivatives in drug delivery, the coordinated environment of compound **7** structurally resembles that of cisplatin. After reductive cleavage from B$_{12}$, the released Pt(II) complex was likely to possess one ammonia and one cyanide ligand and two chlorides, respectively, in *cis* orientation. The chlorides can potentially be replaced by, e.g., N7 from guanines in DNA to exert a cisplatin-like cytotoxic activity. The syntheses of model complexes such as [PtCl$_2$(CN)(NH$_3$)]$^-$ has not been described yet, but was the subject of theoretical studies only [38]. Cisplatin-like activity would probably not be expected for the Pt(II) complex cleaved from **5** because it possesses only one chloride. Platinum in conjugate **6** has two chloride ligands but in *trans* orientation to each other. Transplatin complexes are in general much less active than cisplatin, although some exceptions have been reported [39, 40]. The activity of these monocyano complexes and the influence on the other ligands bound to platinum remain to be investigated in more detail with model complexes.

A platinum complex bound to cyanide in B$_{12}$ with no ammonia but chloride ligands only completed this series.
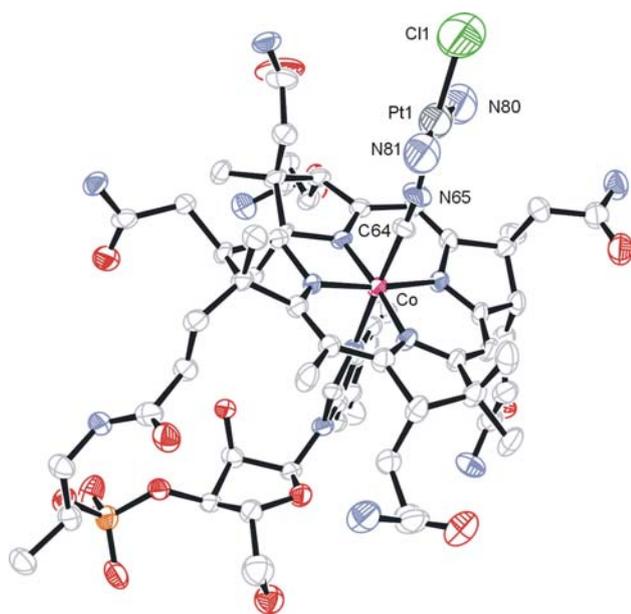
Fig. 3 ORTEP presentation of **5**, selected bond lengths (angstrom) and angles (degree): Co–C64 1.938(9), C64–N65 1.010(11), Pt1–N65 1.991(9), Pt1–N81 1.856(14), Pt1–N80 2.092(15), Pt1–Cl1 2.236(8), N81–Pt1–N80 166.0(7), C64–N65–Pt1 171.0(10), N65–C64–Co 175.0(9). Solvent molecules and hydrogen atoms were omitted for clarity
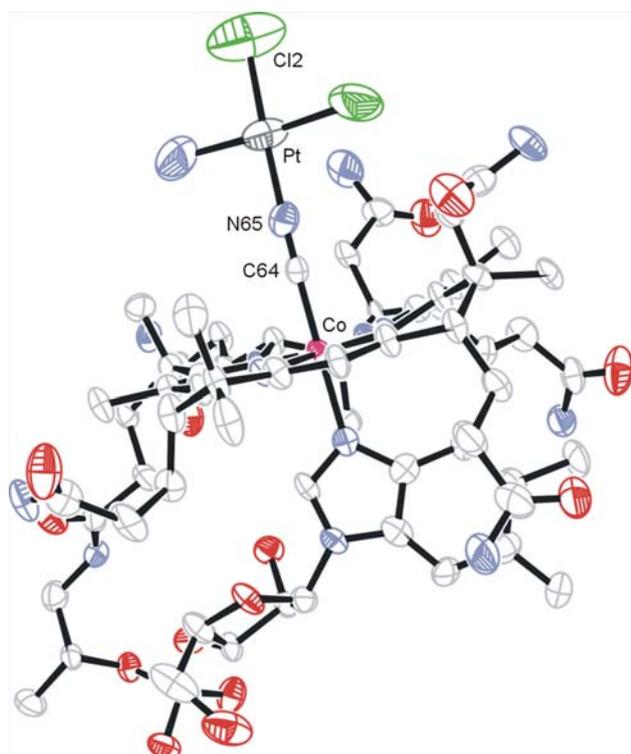

Fig. 4 ORTEP presentation of [{Co}–CN–{*cis*-PtCl₂(NH₃)}] (**7**), selected bond lengths (angstrom) and angles (degree): Co–C64 1.885(10), C64–N65 1.151(13), N65–Pt 1.940(10), Cl2–Pt 2.258(8), N65–C64–Co 178.2(10), C64–N65–Pt 174.5(9). Solvent molecules and hydrogen atoms were omitted for clarity

The reaction of $[PtCl_4]^{2-}$ with B_{12} in methanol was monitored by HPLC. After 10 days of reaction at room temperature, only small amounts of free B_{12} (besides some unidentified side products) were detected. One main signal indicated the formation of **8**, which could be isolated in 35% yield by preparative HPLC. At higher temperatures, the reaction rate or yield did not increase owing to the reactivity of $[PtCl_4]^{2-}$. The amount of side products increased since **8** started to decompose at elevated temperature. Crystals were obtained by vapor diffusion (H_2O/acetone). X-ray analysis confirmed the authenticity [{Co}–CN–{PtCl₃}]⁻ of **8** but the overall quality was not good enough for a detailed discussion.

The electrochemical properties of **5**, **6** and **7** are crucial for the sequence of reactions leading to corrinoid adenosylation [i.e., Co(III) → Co(II) → Co(I) → AdoCbl]. As stated elsewhere, the conjugation of *cis*-[PtCl₂(NH₃)₂] to B_{12} to yield **2** substantially facilitated the reduction of Co(III) to Co(II) [25]. Whilst B_{12} exhibited a reduction wave at $E_{1/2} = -670$ mV (vs. Ag⁺/AgCl) with about 60% reversibility, reduction of compound **5** was shifted toward more positive potentials with $E_{1/2} = -486$ mV and reversibility comparable to B_{12}. Compounds **6** and **7** had similar potentials at $E_{1/2} = -605$ and -584 mV, respectively. The cyclic voltammograms of both compounds **6** and **7** exhibited a high reversibility of 96%. A typical cyclic voltammogram for B_{12} and **5** is depicted in Fig. 5. Obviously, the Co(III) centers in **5**, **6** and **7** are easier to reduce than in B_{12}. Formally, **5** is positively charged at the platinum center, whereas it is neutral in **6** and **7**. The electron-withdrawing Pt(II) center reduces the electron donation from cyanide to Co(III) and renders it more electron poor. Its oxidation potential will consequently increase as observed. Positively charged conjugate **2** fits in this sequence with a reduction potential of -515 mV. A shift of the electrochemical potentials toward more positive values supports thermodynamically the attempted enzymatic reduction in the adenosylation assay.

Stability in BSA solution

For application under physiological conditions, the serum stability of Pt(II)–B_{12} conjugates is essential. It is well known that cisplatin and transplatin bind very rapidly and essentially irreversible to human serum albumin (HSA) [41]. The binding of platinum complexes to HSA has been the subject of many studies and it has been shown that cysteine, which is abundant in HSA, is the most favorable site for coordination [42, 43]. Different kinds of interactions of compounds **5**, **6**, **7** and **8** with serum proteins are possible. Noncovalent lipophilic binding is usually a fast and reversible process detectable shortly after incubation.

Table 1 Crystal data and structure refinement for [{Co}–CN–{*trans*-PtCl(NH$_3$)$_2$}]$^+$ (**5**) and [{Co}–CN–{*cis*-PtCl$_2$(NH$_3$)}] (**7**)

	5	7
Formula	C$_{65}$H$_{115}$Cl$_2$CoN$_{17}$O$_{23}$PPt	C$_{66}$H$_{108}$Cl$_2$CoN$_{15}$O$_{23}$PPt
M_r	1,858.63	1,835.56
Crystal system	Orthorhombic	Orthorhombic
Space group	$P2_12_12_1$	$P2_12_12_1$
a (Å)	15.7056(7)	15.8726(7)
b (Å)	22.4115(14)	22.0230(13)
c (Å)	25.5714(11)	26.2190(14)
α (°)	90	90
β (°)	90	90
γ (°)	90	90
V (Å^3)	9,000.8(8)	9,165.2(8)
Z	4	4
ρ_{calcd} (Mg m^{-3})	1.372	1.330
μ (mm^{-1})	1.888	1.852
F (000)	3,848	3,788
Crystal size (mm^3)	0.61 × 0.12 × 0.10	0.86 × 0.12 × 0.12
θ range (°)	1.98–25.00	1.76–24.14
Index ranges	−18 ≤ h ≤ 18	−18 ≤ h ≤ 17
	−26 ≤ k ≤ 26	−25 ≤ k ≤ 25
	−30 ≤ l ≤ 30	−30 ≤ l ≤ 30
Reflections collected	65,286	59,906
Independent reflections	15,846 [R(int) = 0.0959]	14,396 [R(int) = 0.0860]
Completeness (%)	99.8 (to θ = 25.00°)	98.2 (to θ = 24.14°)
Max/min transmission	0.8337/0.3922	0.8378/0.7363
Data/restraints/parameters	15,846/25/984	14,396/1/964
Goodness of fit on F^2	1.004	1.042
Final R indices [$I > 2\sigma(I)$][a,b]	R1 = 0.0984, wR$_2$ = 0.2617	R1 = 0.0892, wR$_2$ = 0.2325
R indices (all data)[a,b]	R1 = 0.1287, wR$_2$ = 0.2840	R1 = 0.1053, wR$_2$ = 0.2434
Absolute structure parameter	0.005(11)	0.033(9)
Largest diffraction peak/hole (e Å^{-3})	0.997/−1.712	2.194/−1.127

[a] R1 = $\Sigma||F_o| - |F_c||/\Sigma||F_o|$

[b] wR$_2$ = $\{\Sigma[w(F_o^2 - F_c^2)^2]/\Sigma[w(F_o^2)^2]\}^{1/2}$

Covalent and therefore essentially irreversible binding through coordination to platinum by chloride exchange is slow and evolves with time as observed for cisplatin. Such
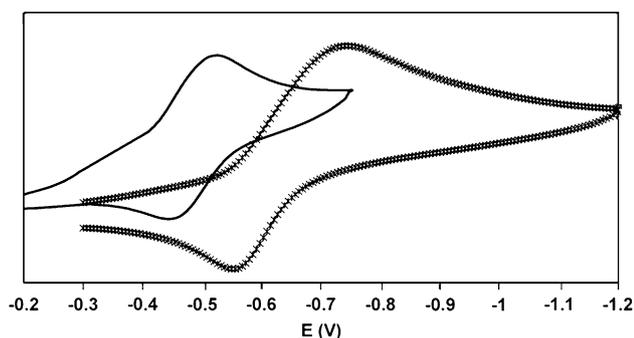

Fig. 5 Cyclic voltammogram of conjugate **5** (*solid lines*) and B$_{12}$ (*crossed lines*). The concentration of the compounds was 1 mM in MeOH with 0.1 M Bu$_4$NPF$_6$ as an inert electrolyte (vs. Ag$^+$/Ag)

interactions can occur with or without cleavage from B$_{12}$ (transmetallation by binding to the cyano position). The appearance of free B$_{12}$ would be indicative for the former decomposition pathway. It should be noted here that free B$_{12}$ has almost no interaction with serum proteins and only 1–2% binds (noncovalently) very rapidly after incubation. This fraction remains constant over time. Less likely, but to be considered owing to the increased electrophilicity of Co(III) in **5**, **6**, **7** and **8**, is the direct attack to Co(III) and cleavage of a complex such as *trans*-[Pt(NC)Cl(NH$_3$)$_2$] from **5**. The formation of HOCbl should be observed for this way of decomposition. Besides potential coordinating sites from proteins, the tripeptide glutathione (GSH) might be prone to these processes as well. Present in high concentrations in human cells [44], GSH spontaneously forms glutathionylcobalamin with HOCbl but not with B$_{12}$ [45]. The availability of unbound B$_{12}$ conjugates **5**, **6**, **7** and **8** over time is crucial for efficient cellular uptake and drug

delivery. We investigated the stabilities under these aspects with two different HPLC systems. Size-exclusion HPLC quantifies the ratio of BSA bound/unbound B_{12} and derivatives. Reversed-phase HPLC accounts for the authenticity of unbound B_{12} conjugates **5**, **6**, **7** and **8**. It should be noted that **5**, **6**, **7** and **8** were stable in pure water and no cleavage or decomposition was observed over several days. The conjugates were incubated in 13 mg mL^{-1} BSA solution and phosphate buffer pH 7.4. The conjugates are more lipophilic than native B_{12}; thus, increased noncovalent binding to proteins was expected. The conjugates **5/7** and **6/8**, respectively, showed qualitatively similar but quantitatively different behavior. Time-dependent stability studies revealed a rapid association with BSA due to noncovalent lipophilic interaction during the first 1–2 h, followed by a smooth increase over the next 48 h. The time dependence of the stability of **7** is given in Fig. 6.

The latter process represents covalent binding to serum proteins. For compounds **5** and **7**, protein association was about 9 and 15% after 48 h in comparison with 2% for native B_{12}. As indicated by the appearance of native B_{12}, transmetallation to BSA was observed in moderate yield. After 48 h, about 25% of free B_{12} with respect to unbound **5** or **7** did form. HOCbl or released platinum complexes were not found because binding to BSA proteins was rapid and efficient [46]. Compounds **6** and **8** showed significantly lower stability. After 24 h, 60% of **6** was bound to the proteins. This decreased stability correlated well with previously described instability of transplatin complexes [47]. Compound **8** decomposed even more rapidly, and to a high degree owing to its increased substitution liability compared with that of the other conjugates. Owing to the instability in BSA solution, **6** and **8** were not included in the subsequent enzymatic studies. Typical HPLC traces for compound **5** after 48 h in BSA solution are given in Fig. 7.

The observed behavior for compounds **5** and **7** assessed their reasonable stabilities in the presence of BSA. The low concentrations of free B_{12} indicated transmetallation to a
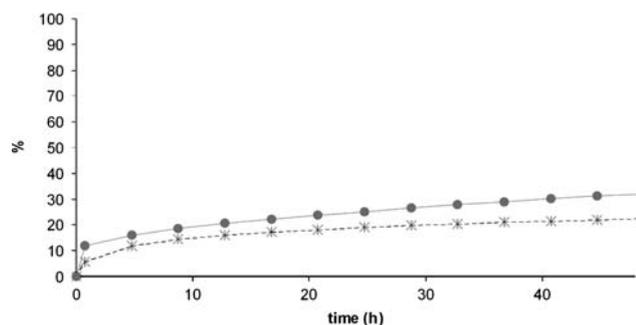

Fig. 6 Percentage of **7** bound to bovine serum albumin (BSA) versus time (*stars*) and formation of B_{12} from **7** in the presence of BSA (*circles*)
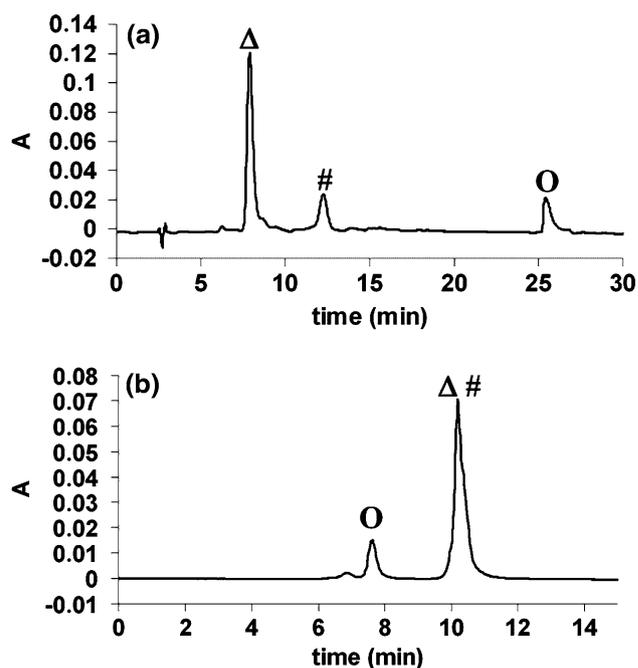

Fig. 7 High-performance liquid chromatography (HPLC) traces of **5** in BSA solution monitored at 360 nm after 24 h. **a** RP-C18 column for the analysis of B_{12} compounds, starting material **5** (*triangle*) decomposition product free B_{12} (*hash*) and cobalamin bound to BSA (*circle*). **b** Size-exclusion HPLC column, all cobalamins bound to BSA proteins (*circle*), and free cobalamins (*triangle*, *hash*)

small extent. Since HOCbl binds very fast to histidine side chains of BSA proteins, HOCbl, if ever formed, was not observed for any compound [48].

Enzymatic adenosylation

After TCII receptor-mediated endocytosis, B_{12} is released from TCII. To become functionally active, B_{12} and its derivatives are either adenosylated in mitochondria or methylated in the cytoplasm to become the respective cofactors for methylmalonylcoenzyme A mutase or methionine synthase. If the platinum complexes were activated by cleavage from B_{12}, compounds **5** and **7** would be recognized and processed by the enzymes of the corrinoid adenosylation pathway. The corrinoid adenosylation system used in this work required the flavin mononucleotide dependent reductase, the electron-transfer protein flavodoxin (FldA) and the ferredoxin Fpr as reductases for the steps Co(III) → Co(II) and Co(II) → Co(I), respectively. Co(I) was adenosylated by the *S. enterica* CobA enzymes using ATP as a cosubstrate via an oxidative addition. Theoretical calculations based on these sequential processes were in agreement with corresponding experimental data [49]. It should be emphasized here that in humans B_{12} is an unfavorable entry into this process

because the cyanide ligand has to be replaced by H_2O or OH^- with the help of a β-ligand transferase; the identity of the latter enzyme is unknown [50, 51]. Only HOCbl would be converted to AdoCbl. The corrinoid adenosylation assay is sketched in Scheme 2.

For the purpose of targeted metal complex delivery to, e.g., cancer cells, the first reductive process Co(III) → Co(II) is decisive. Upon reduction of Co(III) to Co(II) the β axial ligand, in this study the platinum complexes, is released [52, 53]. After reduction, cob(II)alamin enters the second reduction Co(II) → Co(I) and finally adenosylation. Although only the first process is the basis for drug delivery, the formation of AdoCbl is an experimental indication for cleavage of the platinum complexes and has also been studied. As mentioned earlier, an in vitro reducing system for the enzymatic conversion of HOCbl to AdoCbl has been reported previously and we used this system for assessing the formation of AdoCbl from 5 and 7 [7, 54].

The corrinoid adenosylation process can be subdivided into three different steps. The respective activities and rates have been investigated for 5 and 7 and the "blank" compounds B_{12} and HOCbl. The first two reduction steps can be mimicked by reducing 5 and 7 chemically with $[BH_4]^-$ (step iv in Scheme 2). Co(I)Cbl has a distinct UV/vis spectrum with an indicative band at 385 nm. Co(I)Cbl chemically generated from, e.g., 5 by $[BH_4]^-$ reduction was then catalytically converted by CobA to AdoCbl at a comparable rate to the one found for the natural substrate cob(I)alamin generated from HOCbl. The UV/vis spectrum after $[BH_4]^-$ reduction of 5 and the subsequent AdoCbl spectrum after adenosylation with CobA were identical to the spectra from authentic samples after full enzymatic conversion (see below).

On the basis of the measured reduction potentials, it was not surprising that 5 and 7 were rapidly reduced by $[BH_4]^-$. More interesting was the question of whether 5 and 7 were

reduced by the FldA–Fpr system. Owing to the characteristic UV/vis bands of B_{12} in the different oxidation states, the stepwise process was monitored spectroscopically. Typical spectra for the time course of reduction of HOCbl, 5 and 7 from Co(III) to Co(II) in the FldA–Fpr system are shown in Fig. 8.

This assay clearly showed that compounds 5 and 7 were reduced and converted to cob(II)alamin by the reductases despite the presence of a relatively large metal complex bound to the respective cyanide. It should also be noted that B_{12} is a very bad substrate for this reduction process and reacted at a substantially lower rate than compound 5, for example. The rate of these reduction processes showed half-life times for HOCbl to be less than 10 s, 17 min for 5 and 65 min for 7, whereas the reduction of B_{12} was not finished even after 24 h. The reduction potential of B_{12} is −670 mV. whereas the ones of H_2OCbl and 5 are −200 and −486 mV, respectively [52, 53]. The same behavior was also observed in electrochemical reduction. A spectroelectrochemical assay was set up in order to mimic the in vitro corrinoid adenosylation process. Reduction under the same conditions (0.2 M Tris buffer, pH 8, 37 °C, 800 μM $MgCl_2$ and 50 μM of the corresponding cobalamin) but now with a continuous potential of −700 mV revealed a comparable conversion. Typical UV/vis spectra for the electrochemical reduction of Co(III) to Co(II) for HOCbl, B_{12} and 7 are shown in Fig. 9. For the enzymatic and the electrochemical reduction process, reoxidation of cob(II)alamin with air gave exclusively HOCbl, implying the cleavage of the platinum complex together with the cyanide ligand from cobalt.

When compound 5 was reduced in the FldA–Fpr system to Co(II) but in the absence of CobA, further reduction to cob(I)alamin and oxidative addition of ATP to AdoCbl was not observed. Only addition of CobA and ATP lead to the reduction of Co(II) to Co(I) in the active site of the CobA enzyme followed by a nucleophilic attack of C5′ of the

Scheme 2 Corrinoid adenosylation pathway: electrons for reduction of cob(III)alamin to cob(I)alamin are donated by NADPH through flavodoxin protein. *i* Dihydroflavins or Fpr–FADH$_2$, *ii* FldA–FMNH$^+$, *iii* CobA, *iv* KBH$_4$
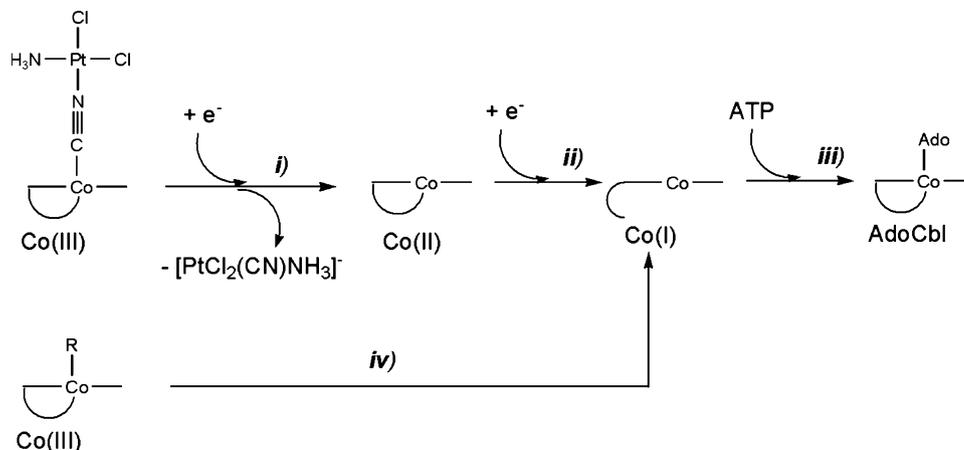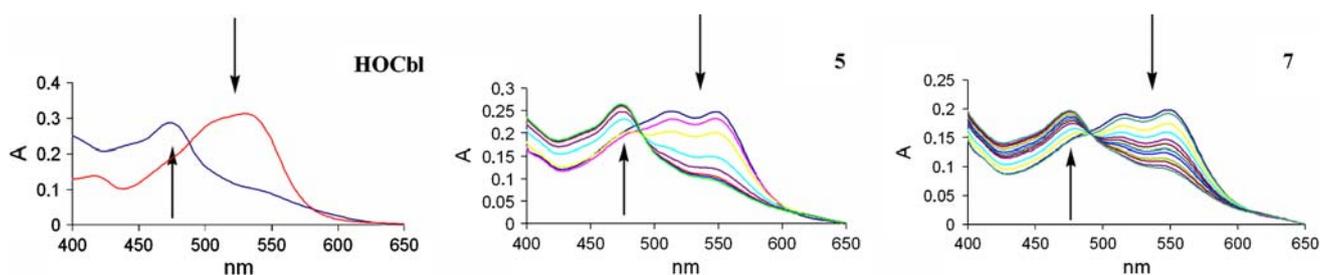
Fig. 8 Reduction of aqua-cobalamin (HOCbl), **5** and **7** using FldA–Fpr proteins. Spectral changes were associated with the conversion of cob(III)alamin to cob(II)alamin; UV/vis spectra of **5** and **7** recorded in 10-min intervals. The last spectrum with $\lambda_{max} = 470$ nm is that of the cob(II)alamin solution
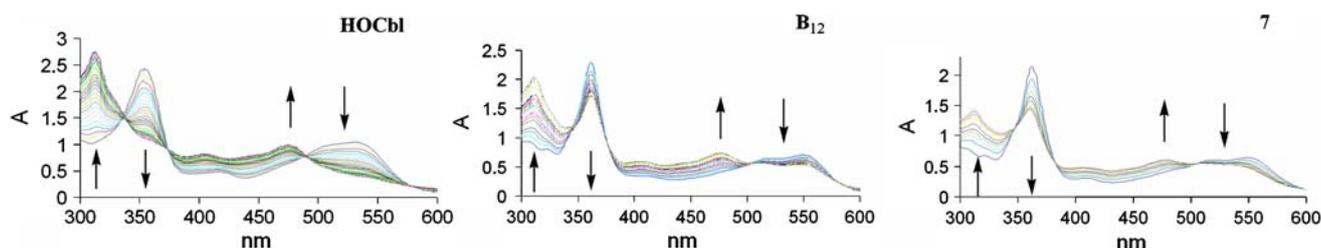

Fig. 9 Spectral changes associated with the conversion of cob(III)alamin to cob(II)alamin at $E = -700$ mV. UV/vis spectra of HOCbl every 10 min; UV/vis spectra of a solution of B_{12} and **7** every 1 h [measurements of B_{12} and **7** were stopped before full conversion to Co(II)]

ribosyl moiety of ATP, resulting in the formation of AdoCbl and the release of triphosphate. A series of UV/vis spectra for the adenosylation process with **5** and **7** are shown in Fig. 10.

As mentioned previously, the Co(III) → Co(II) reduction process with the FldA–Fpr system was slower for **5** and **7** than for HOCbl but much faster than for B_{12}. If the platinum complexes as β axial ligands were released in the reduced cob(II)alamin, the adenosylation step should occur at rates comparable to those for HOCbl. Indeed, this was the case, and about 30 min after addition of CobA and ATP, AdoCbl formed quantitatively. Although present in relatively large concentrations (see "Materials and methods"), the Pt(II) complexes released from **5** or **7** did not affect the rate of these processes, probably owing to the relatively short time periods of observation.

The final product of the full adenosylation assay starting from **5** or **7** was isolated by HPLC. To assess its nature as AdoCbl, its biological activity on the growth of *S. enterica* was investigated. Strain JE7179 is a standard for these tests of biological activity since these cells do not produce CobA. Therefore, strain JE7179 only grew if AdoCbl was present in the culture medium. Strong growth was observed when authentic AdoCbl or the product of the adenosylation assay of **5** or **7** was provided to the indicator strain. Strong growth was also observed with AdoCbl generated in KBH_4-dependent adenosylation assays using **5** or **7** as the substrate. As expected, no growth was observed with pure B_{12} or HOCbl or with the

product isolated from reduction to Co(II) with FldA–Fpr but no subsequent adenosylation. A number of these growth responses are shown in Fig. 11.
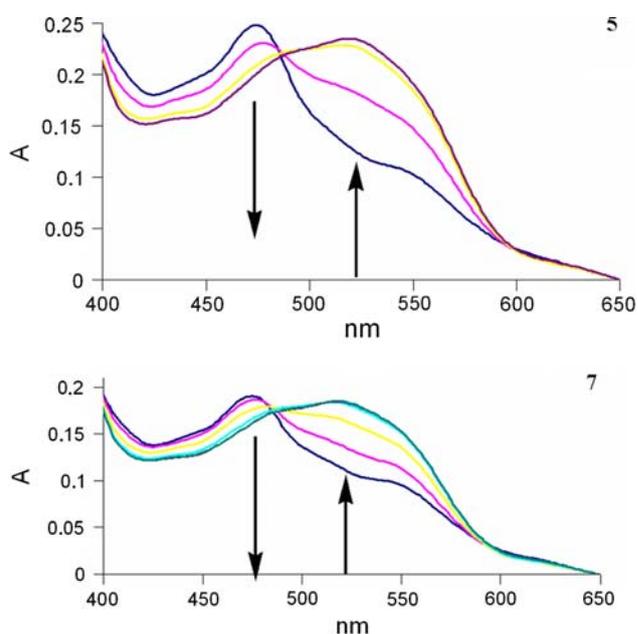

Fig. 10 Spectral changes associated with the conversion of cob(II) alamin prepared from **5** and **7** in the first reduction step to adenosylcobalamin (AdoCbl): solution of cob(II)alamin directly after addition of CobA monitored every 10 min (in the case of **5**) or every 5 min (in the case of **7**)
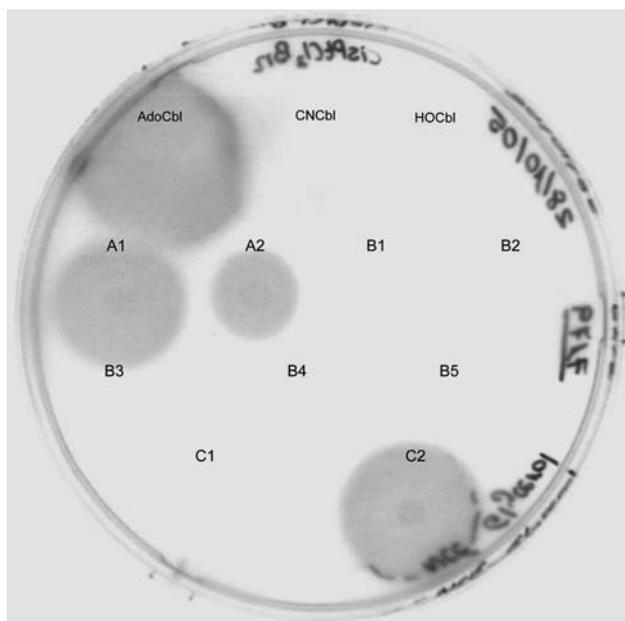
Fig. 11 In vivo assessment of AdoCbl formation. Controls for the growth response: AdoCbl, B$_{12}$ (*CNCbl*), HOCbl. *A* AdoCbl isolated from HPLC after reaction of **7** with FldA + Fpr and CobA. *B* Peaks separated from HPLC after reaction of **7** with FldA–Fpr only. *C* Peaks isolated from HPLC after reaction of **7** with [BH$_4$]$^-$ and adenosylation with CobA

Conclusion

We have synthesized and characterized the four heterodinuclear conjugates **5**, **6**, **7** and **8** in which B$_{12}$ acts through its cyanide group as a ligand to a variety of Pt(II) complexes. To be released, the platinum complexes have to be cleaved from B$_{12}$. We showed with an in vitro adenosylation assay from *S. enterica* that Co(III) is reduced to Co(II) with the concomitant cleavage of the Pt(II) complexes. This is essential for the use of B$_{12}$ as a drug delivery carrier for cisplatin-like compounds such as **7** where the two chloride ligands are reminiscent of cisplatin. Although only this first step is decisive for the role as a drug carrier, the B$_{12}$-based products underwent a further one-electron reduction Co(II) → Co(I) and subsequent adenosylation to AdoCbl in the complete enzymatic assay. Since the B$_{12}$ conjugates described here are still converted by the corresponding enzymes, B$_{12}$ might serve as a carrier for cytotoxic substances. The nature of the Pt(II) complexes released, their cytotoxicity and the effect on cancer cell lines is under investigation.

References

1. Warren MJ, Raux E, Schubert HL, Escalante-Semerena JC (2002) Nat Prod Rep 19:390–412
2. Norberg B (1999) J Intern Med 246:237–238
3. Okuda K (1999) J Gastroenterol Hepatol 14:301–308
4. Chanarin I (2000) Br J Haematol 111:407–415
5. Seetharam B, Bose S, Li N (1999) J Nutr 129:1761–1764
6. Fonseca MV, Buan NR, Horswill AR, Rayment I, Escalante-Semerena JC (2002) J Biol Chem 277:33127–33131
7. Fonseca MV, Escalante-Semerena JC (2001) J Biol Chem 276:32101–32108
8. Fonseca MV, Escalante-Semerena JC (2000) J Bacteriol 182:4304–4309
9. Hall DA, Vander Kooi CW, Stasik CN, Stevens SY, Zuiderweg ERP, Matthews RG (2001) Proc Natl Acad Sci USA 98:9521–9526
10. Walker GA, Murphy S, Huennekens FM (1969) Arch Biochem Biophys 134:95–105
11. Boyle SM, Markham GD, Hafner EW, Wright JM, Tabor H, Tabor CW (1984) Gene 30:129–136
12. St. Maurice M, Mera PE, Taranto MP, Sesma F, Escalante-Semerena JC, Rayment I (2007) J Biol Chem 282:2596–2605
13. Buan NR, Escalante-Semerena JC (2006) J Biol Chem 281:16971–16977
14. Johnson CL, Buszko ML, Bobik TA (2004) J Bacteriol 186:7881–7887
15. Suh S, Escalante-Semerena JC (1995) J Bacteriol 177:921–925
16. Bauer CB, Fonseca MV, Holden HM, Thoden JB, Thompson TB, Escalante-Semerena JC, Rayment I (2001) Biochemistry 40:361–374
17. Cannon MJ, Myszka DG, McGreevy JM, Holden JA, West FG, Grissom CB (2001) FASEB J 15:A556–A556
18. Smeltzer CC, Cannon MJ, Pinson PR, Munger JDJ, West FG, Grissom CB (2001) Org Lett 3:799–801
19. Grissom CB, Horton RA, McCain K, Harris JM (2005) FASEB J 19:A833–A833
20. Bagnato JD, Eilers AL, Horton RA, Grissom CB (2004) J Org Chem 69:8987–8996
21. Horton RA, McCain KS, Harris JM, Grissom CB (2005) Biophys J 88:264A–264A
22. Collins DA, Hogenkamp HPC, O'Connor MK, Naylor S, Benson LM, Hardyman TJ, Thorson LM (2000) Mayo Clin Proc 75:568–580
23. Russell-Jones G, McTavish K, McEwan J, Rice J, Nowotnik D (2004) J Inorg Biochem 98:1625–1633
24. Kunze S, Zobi F, Kurz P, Spingler B, Alberto R (2004) Angew Chem Int Ed 43:5025–5029
25. Mundwiler S, Spingler B, Kurz P, Kunze S, Alberto R (2005) Chem Eur J 11:4089–4095
26. Lippert B (1999) Cisplatin: chemistry and biochemistry of a leading anticancer drug. Helvetica Chimica Acta, Zurich
27. Kraker AJ, Hoeschele JD, Elliott WL, Showalter HDH, Sercel AD, Farrell NP (1992) J Med Chem 35:4526–4532
28. STOE & Cie (1999) CELL. STOE & Cie, Darmstadt
29. Altomare A, Burla MC, Camalli M, Cascarano GL, Giacovazzo C, Guagliardi A, Moliterni AGG, Polidori G, Spagna R (1999) J Appl Crystallogr 32:115–119
30. Sheldrick GM (1997) University of Göttingen, Germany
31. Berkowitz D, Hushon JM, Whitfield HJJ, Roth J, Ames BN (1968) J Bacteriol 96:215–220
32. Fanchiang YT, Bratt GT, Hogenkamp HPC (1983) J Chem Soc Dalton Trans 1929–1934
33. Bax A, Marzilli LG, Summers MF (1987) J Am Chem Soc 109:566–574

34. Brown KL, Hakimi JM, Jacobsen DW (1984) J Am Chem Soc 106:7894–7899
35. Hamza MSA, Zou X, Brown KL, van Eldik R (2001) Inorg Chem 40:5440–5447
36. Nakamoto K (1978) Infrared and Raman spectra of inorganic and coordination compounds, 3rd edn. Wiley, New York
37. Spingler B, Mundwiler S, Ruiz-Sánchez P, van Staveren DR, Alberto R (2007) Eur J Inorg Chem 2641–2647
38. Armstrong DR, Fortune R, Perkins PG (1974) Inorg Chim Acta 9:9–18
39. Montero EI, Perez JM, Schwartz A, Fuertes MA, Malinge JM, Alonso C, Leng M, Navarro-Ranninger C (2002) ChemBioChem 3:61–670
40. Khazanov E, Barenholz Y, Gibson D, Najajreh Y (2002) J Med Chem 45:5196–5204
41. DeConti RC, Toftness BR, Lange RC, Creasey WA (1973) Cancer Res 33:1310–1315
42. Trynda-Lemiesz L, Keppler BK, Kozlowski H (1999) J Inorg Biochem 73:123–128
43. Ivanov AI, Christodoulou J, Parkinson JA, Barnham KJ, Tucker A, Woodrow J, Sadler PJ (1998) J Biol Chem 273:14721–14730
44. Zhao R, Lind J, Merenyi G, Eriksen TE (1997) J Chem Soc Perkin Trans 2:569–574
45. Xia L, Cregan AG, Berben LA, Brasch NE (2004) Inorg Chem 43:6848–6857
46. Cole WC, Wolf W (1980) Chem Biol Interact 30:223–235
47. Trynda-Lemiesz L, Kozlowski H, Keppler BK (1999) J Inorg Biochem 77:141–146
48. Taylor RT, Hanna ML (1970) Arch Biochem Biophys 141:247–257
49. Stich TA, Buan NR, Escalante-Semerena JC, Brunold TC (2005) J Am Chem Soc 127:8710–8719
50. Pezacka E (1993) Biochem Biophys Acta 1157:167–177
51. Johnson CLV, Buszko ML, Bobik TA (2004) J Bacteriol 186:7881–7887
52. Lexa D, Saveant JM (1976) J Am Chem Soc 98:2652–2658
53. Lexa D, Saveant JM, Zickler J (1977) J Am Chem Soc 99:2786–2790
54. Suh SJ, Escalante-Semerena JC (1995) J Bacteriol 177:1918–1918